Design, and Experimental Investigation of indirect solar thermal cooker for street food cooking

Zelalem Teshome[1] and Abdulkadir Aman Hassen[2*],

[1] School of Mechanical and Industrial Engineering, Dire Dawa University, Institute of Technology, Dire Dawa, Ethiopia

[2] School of Mechanical and Industrial Engineering, College of Technology and Built Environment, Addis Ababa University, Addis Ababa, Ethiopia

Abstract

This work delves into the working principles of solar cookers, leading to the design of one with an asymmetric CPC (Compound Parabolic Collector). The study commences by assessing potato chip frying methods in Dire Dawa city to determine the energy required for frying, aiding in the solar cooker component design. Subsequently, data collection is followed by methodological planning for experimentation, optimizing thermal balances for various components. A solar cooker prototype is then designed and manufactured, with performance parameters evaluated through experiments and MATLAB simulations, showing slight discrepancies. Further analysis investigates reasons for variations, followed by model validation and performance assessment. Results indicate the constructed cooker as an A-Grade solar cooker, with high optical efficiency of the glass plate and low radiation losses from the side walls. The cooker exhibits good heat transfer capacity with a cooking power of 29.1 W and an efficiency of 17.24%, indicating room for improvement in selected solar parameters. The system's return on investment is estimated at 2 years.

Keywords: Compound Parabolic Concentrators, Absorber Plate, Thermal Energy Storage, MATLAB simulation.

1. Introduction

The escalating energy demand driven by industrial expansion and population growth has underscored the urgency of exploring alternative energy solutions amid mounting concerns over global warming and environmental degradation. While fossil fuels have historically fueled economic progress, their environmental impact has spurred a shift towards renewable energy sources. Renewable energy, deemed crucial for future energy developments, offers a sustainable substitute to traditional sources.

Cooking, a fundamental household activity globally, heavily relies on fossil fuels in developing nations, leading to deforestation and health risks from smoke exposure. Solar thermal energy emerges as a promising alternative to reduce dependence on fossil fuels, particularly in areas with limited access to electricity. Renewable energy technologies, notably solar power, provide a commercially viable and eco-friendly energy source rooted in natural phenomena.

The study endeavors to address these challenges by investigating the design, construction, and experimental evaluation of an indirect solar thermal cooker tailored for street food preparation. Through optimizing Compound Parabolic Collector (CPC) designs and integrating advanced heat transfer mechanisms, the study aims to enhance the efficiency of solar cookers. Employing a systematic methodology involving literature review, conceptual design development, and numerical optimization of thermal balances, the study aims to fabricate a functional prototype for practical assessment.

By advancing sustainable cooking technologies through solar cookers, the study seeks to mitigate carbon emissions, enhance energy accessibility in underserved regions, and foster environmental sustainability. The research outcomes hold potential to inform policymakers, engineers, and designers on the adoption of solar cookers worldwide, facilitating a transition towards environmentally conscious cooking practices and contributing to a greener future.

10.18086/swc.2025.02.12 Available at http://proceedings.ises.org

1.1. Solar thermal cooker for street food cooking

Due to their ease of handling and operation, box type solar cookers are more popular among direct solar cookers (V. Thirunavukkarasu, 2020). There are various box-style solar cooker designs available to improve the solar cooker's thermal performance. The design of the cooker pot also contributes to enhancing the cooker's thermal efficiency. Alozie et al. have designed, built, and tested a solar box cooker to see if it can successfully cook food in most tropical regions where there is an abundance of solar radiation (E.W. Gabisa, 2016).

The box's interior has been painted black to enhance its ability to absorb sunlight. The box can hold up to four cooking vessels (H. El Hage, 2018). Typically, the box's cover has a two-pane "window" that allows light from the sun to enter while preventing heat from escaping. This is in addition to a mirror-embedded lid that can be adjusted to enhance the box's insulation when closed and intensify incident radiation when it is open (S. Indora, 2018). The thermal efficiency and design of the cooker determine how quickly food cooks.

The increasing concerns related to energy security combined with excessive waste of useful energy have resulted in the development of a variety of energy-efficient technologies to meet the energy demand in the major energy sectors including industry, transport, construction, and buildings (R. Wimmer, 2017). Thermal energy storage (TES), or thermal storage, is the one competent technology existing that provides to end-use energy demand through energy redistribution (A.A. Sagade, 2021). A box-style solar cooker with a finned absorber was the subject of an experimental investigation by Mostafa Zakariapour and Muhammadreza Sedighi (Mohammadreza Sedighi, 2014). According to the findings, a solar box cooker with fins was roughly 7% more efficient than a solar cooker without any fins. Using a finned absorber plate decreased the amount of time needed to bring water to a boil by roughly 12%. The impact of sand and granular carbon, which were used as the heat-absorbing material on the absorber plate surface of the solar box cooker, was investigated experimentally (A.H. Tesfay, 2019).

A compound parabolic concentrator is a non-focusing type of concentrating collector that provides a moderate concentration of solar radiation, albeit less than a focusing collector. It only needs a few tilt adjustments per year and does not require continuous solar tracking (A.G. Bhave, 2018). Optical devices called compound parabolic concentrators (CPCs) are used to effectively gather and focus light onto a smaller area. They are frequently utilized in solar-powered appliances like solar cookers and water heaters. Because of its unique form, CPCs are able to redirect light from a wide range of incoming angles toward a focal point. This design aids in increasing the concentration of energy at the focus point and maximizing the amount of light captured. CPCs are renowned for their exceptional optical efficiency and capacity to focus light in less-than-ideal environments (MAWIRE, 2019).

Due to their low cost of materials and ease of manufacture, solar panel cookers are the most widely available type of solar cookers (A.H. Elsheikh, 2019). They use reflective mirrors to focus sunlight onto a cooking vessel that is housed inside a transparent plastic bag. For economical CPC coatings, aluminum is frequently advised for the following reasons: Cost: When compared to other reflective materials like silver, aluminum is comparatively less expensive (A. Herez, 2018). Similarly, an essential property for capturing solar energy is aluminum's high reflectivity over a wide wavelength range, especially in the visible and near-infrared regions. It maximizes the performance of the solar cooker by effectively reflecting solar radiation onto the cooking area (Senthil, 2020). Moreover, the ability of aluminum coatings to withstand environmental conditions and remain strong is well-known. It doesn’t significantly deteriorate when exposed to sunlight, temperature changes, or humidity. This robustness guarantees the CPC will last longer and lowers the need for frequent maintenance or recoating (H.A. Zafar, 2018).

2. Methods and Materials

2.1. Design of Asymmetric CPC

In order to install a box-type solar cooker with an asymmetric CPC at Dire Dawa University in Dire Dawa City, the best design should be at latitude 9.6208°, or 9° 37' 15" north, and longitude 41.84182°, or 41° 50' 31" east and has an altitude of 1154 meters. This configuration must maximize solar irradiation who reaches the absorber plate during a period of 5 h around solar noon starting at 9 AM.

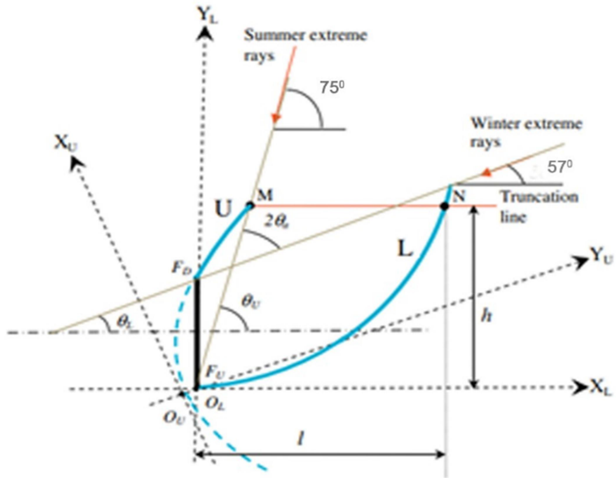

Figure 1 Geometry of the asymmetric CPC for a box-type solar

The absorber plate must be able to intercept all solar rays of which the altitude angle is between solar altitude angle at 9 AM in December and solar altitude angle at noon in June. Calculations made for Dire Dawa give: 75.69° for the maximum solar altitude angle and 56.72° for the minimum solar altitude angle. For practical values, we take 75° and 56° . As shown on Fig. 1, the collector intercepts all solar rays between $\theta_L = 56°$ and $\theta_U = 75°$.

Acceptance Angle is the limiting angle over which incident ray path may deviate from normal to the aperture plane and still reach the absorber.

$$2\theta_c = \theta_L - \theta_U = 75° - 56° = 19° \quad \text{(eq. 1)}$$

The geometrical concentration ratio will be:

$$C = \frac{1}{\sin\ _{c}} = \frac{1}{\sin(9.5°)} = 6 \quad \text{(eq.2)}$$

The height of lower parabola is given as:

$$h^L = [W + \left(\frac{2W}{1-\sin\theta_L}\right)\cos\theta_L \sin\theta_L] \quad \text{(eq. 4)}$$

The distance between the foci of the two parabolas is equal to the absorber plate width (W_r). To specifically decide the dimension of the width of the receiver (absorber) we take an assessment of the standard sizes of potato frying machine, based on the assessments taken almost all machines with single frying tank have similar dimensions. For this study we used the width of the frying tanks as 205 mm.

$$h^L = \left[W + \left(\frac{2W}{1-\sin\theta_L}\right)\cos\theta_L \sin\theta_L\right] = 695\text{mm} \quad \text{(eq. 5)}$$

The length of lower parabola is given as:

$$l^L = \left(\frac{2W}{1-\sin\theta_L}\right)\cos\theta_L = 755\text{mm} \quad \text{(eq. 6)}$$

The height of upper truncated parabola is given as:

$$h^U = \left[\left(\frac{W(1-\sin 124)}{1-s\quad(\theta_U+3\ )}\right)\cos(90-\theta_U)\right] = 399.14 \quad \text{(eq. 7)}$$

The length of upper parabola is given as:

$$l^U = \left[\left(\frac{W(1-\sin 124)}{1-s\quad(\theta_U+34)}\right)\sin(90-\theta_U)\right] = 70.32\text{mm} \quad \text{(eq. 8)}$$

With the help of trigonometric relations, the CPC aperture width (Lo) will be calculated by:

$$L_o = \sqrt{(h^L - h^U)^2 + (l^L - l^U)^2} = 745.85\text{mm} \quad \text{(eq. 9)}$$

And the effective geometric concentration ratio (with truncation) will be:

$$C = \frac{L_o}{W} = 3.62 \quad \text{(eq. 10)}$$

2.2. Thermal Energy Balance Equations

Assumption

- All the systems have uniform temperature;
- Reflection from the CPC touches the double glaze plate;
- The absorber plate is heated by solar radiation which crosses the double glazing after concentration by the reflector;
- The absorber plate transmits its heat to the burnt oil by conduction;
- The stored heat in the burnt oil then transmitted to the Aluminum chips, used to store the heat circulated in the box.
- Finally, the heat stored in the aluminum chips would heat the cooking pot contact with aluminum chips.
- Furthermore, during evening cooking, inner material (aluminum chips) transfers its stored heat to the cooking pot while the outer material (burnt oil) helps in compensating the loss to maintain its performance.

2.2.1. Thermal balance equation of the 1st glass of the double glazing

Regarding this thermal balance, the absorbed solar radiation makes up the heat that travels between the first and second glasses via convection and radiation. This heat flow at the inlet is equivalent to the total heat flow in the first glass plus the heat flow dissipated by convection between the first glass and the surrounding air and radiation from the sky. The thermal balance equation for the first glass in the glazing is as follows in terms of heat rates:

$$(MC_P)_{v1}\frac{dT_{v1}}{dt} = S_vG_{v1} + S_v(hr_{v2-v1} + hc_{v2-v1})(T_{v2} - T_{v1}) - S_vh_{r_{v1-s}}(T_{v1} - T_s) - S_vhc_{v2-amb}(T_{v1} - T_{amb}) \quad \text{(eq. 11)}$$

2.2.2. Thermal balance equation of the 2nd glass of the double glazing

A certain amount of solar radiation reaches the first glass, but only τ times as much reaches the second glass. This heat flow is supplemented by the heat flow from the radiation of the absorber plate. Because of the hotter air gap between it and the second glass, convection from the absorber plate causes the second glass to receive more heat flow. The second glass collects some of the heat flow that is received, while convection and radiation across the first glass lose the remaining heat. The formula for the thermal balance of the second glass in the glazing is as follows:

$$(MC_P)_{v2}\frac{dT_{v1}}{dt} = S_vG_{v2} + S_{ab}hr_{ab-v2}(T_{ab} - T_{v2}) - S_vh_{c_{v2-ac}}(T_{v2} - T_{ac}) - S_v(hr_{v2-v1} + hc_{v2-v1}(T_{v2} - T_{v1}) \quad \text{(eq. 12)}$$

2.2.3. Thermal balance equation of the absorber plate

The heat absorbed by the absorber plate, the heat flow through radiation between the absorber and glass 2, the heat flow through conduction between the burnt oil and the absorber plate, and the lost heat flow through the insulation are the only heat flows for the absorber plate that are included in the thermal balance equation. All other heat flows are deemed to be too tiny and insignificant. As a result, the absorber plate's relative thermal balance equation can be expressed as follows:

$$(MC_P)_{ab}\frac{dT_{ab}}{dt} = S_{ab}G_{ab} - S_{ab}hr_{ab-v2}(T_{ab} - T_{v2}) - S_{ab}hk_{ab-b}\ (T_{ab} - T_{bo}) \quad \text{(eq. 13)}$$

2.2.4. *Thermal balance Equation of the burnt oil*

The only heat flows for the burnt oil that are included in the thermal balance equation are the heat flow via conduction between the burnt oil and the aluminum chips and the heat flow between the burnt oil and the absorber plate. as well as the heat lost via the insulation are considered. Consequently, the relative thermal balance equation for the burned oil inside the box is as follows:

$$(MC_P)_{al}\frac{dT_{bo}}{dt} = S_{ab}hk_{ab-bo}(T_{ab} - T_{bo}) + S_{bo}hk_{bo-al}(T_{bo} - T_{al}) - S_{boash}h_{bo-am}(T_{bo} - T_{am}) \quad \text{(eq. 14)}$$

2.2.5. *Thermal balance equation of the Aluminum chips*

The thermal balance equation only considers the following heat flows for aluminum chips: the heat flow rate between the chips and the cooking oil, the heat flow rate between the chips and the burnt oil, and the lost heat flow through the insulation. As a result, the following is the relative thermal balance equation for the aluminum chips inside the box.

$$(MC_P)_{al}\frac{dT_{al}}{dt} = S_{bo}hk_{al-} \quad (T_{bo} - T_{al}) - S_{al}hk_{al-co}(T_{al} - T_{co}) - S_{alash}h_{al-am}(T_{al} - T_{am}) \quad \text{(eq. 15)}$$

2.2.6. *Thermal balance equation of the cooking oil*

Since the heat flow rate between the cooking oil and the aluminum chips and the lost heat flow through the insulation are the only heat flows for the cooking oil that are taken into account in the thermal balance equation, the relative thermal balance equation for the cooking oil inside the box can be written as follows.

$$(MC_P)_{Co}\frac{dT_{co}}{dt} = S_{al}hk_{al-bo}(T_{al} - T_{bo}) - S_{coas}\ h_{co} \quad (T_{co} - T_{am}) \quad \text{(eq. 16)}$$

2.3. Thermal performance of solar cooker

2.3.1. *First Figure of Merit (F_1)*

The first figure of merit (F_1) is defined as the ratio of optical efficiency, (ηo), and the overall heat loss coefficient, (U_L).

$$F_1 = \frac{\eta\text{o}}{\text{U}_\text{L}} = \frac{(T_{v1,max-T_{amb}})}{I_s} \quad \text{(eq. 17)}$$

Where F_1 is first figure of merit (Km2 w−1), ηo is optical efficiency (%), U_L is overall heat loss factor (Wk−1 m−2), T_{v1},max is upper glass maximum temperature (^{0}C), Tamb is Ambient (^{0}C), and I_s is insolation on a Horizontal surface (Wm−2) (Folaranmi, 2013).

2.3.2. *Second Figure of Merit (F2)*

The second figure of merit, F_2, of box type solar cooker is evaluated under full-load condition and can be defined as the product of the heat exchanger efficiency factor (F_2) and optical efficiency (ηo = $\alpha\tau$). It can be expressed as:

$$F_2 = F'\eta\text{o} = \frac{F_1(MC)_W}{Aap(t_f - t_i)} ln\frac{1-(\frac{1}{F_1})(\frac{T_{wi}-T_{amb,av}}{I_{av}})}{1-(\frac{1}{F_1})(\frac{T_{wf}-T_{amb,av}}{I_{av}})} \quad \text{(eq. 18)}$$

Where M is the mass of the load of water inside the solar cooker, C_p, is the specific heat capacity of the load of water $T_{amb,av}$ and I_{av} are respectively the average ambient temperature and the average solar radiation during the test.

2.3.3. Cooking power

For the cooking power calculation, the standard ASAE S580 JAN03 was considered. According to this standard some conditions must be controlled:

$$P_i = mC(T_2 - T_1)$$

Where, P_i = cooking power (W), T_2 = final water temperature, T_1 = initial water temperature, m = water mass (kg), C = heat capacity (4186 J/[kg·K]). The time, 600 seconds represent a ten-minute interval.

The standardized cooking power is calculated by multiplying by the standard insolation of 700W/m^2 and by dividing the recorded solar radiation with in a time interval.

$$p_s = p_i(\frac{700}{I_i})$$

Where, P_s = standardized cooking power (W), Pi = interval cooking power (W), calculated in (3.22), I_i= interval average solar insolation (W/m2). A linear regression of the plotted points shall be used to find the relationship between cooking power and temperature difference in terms of intercept, a (W), and slope, b (W/°C)

$$T_d = T_w - T_a$$

2.3.4. Efficiency

The equation for the efficiency of solar cooker becomes:

$$\eta = \frac{Out\ put\ power}{Input\ power} = \frac{m_w C_{pw} \Delta T}{IAape\Delta t} \quad \text{(eq. 19)}$$

2.4. Experimental setup

2.4.1. Description of the Solar Cooker Prototype

The solar cooker used in the present investigation is of an insulated box equipped with a vertical double glazing cover on one side, a vertical absorber plate laid out just behind a transparent cover and two parabolic reflectors fixed on the glazed side of the box so that solar radiation incident on the horizontal aperture is reflected towards the absorber plate through the glazing. The burnt oil in contact with the absorber plate, warms up by conduction and transmits its heat to the Aluminum chips reside around the interior surface of the box and helps retain and store the optimum heat received inside the box. The stored heat in thermal storage medium in this case burnt oil transmitted to the Aluminum chips used to store the heat in the box. Finally, the heat would heat the cooking pot structure made on the box.

2.4.2. Construction of solar collector and solar cooker with TES

Major experiments have been conducted, to investigate the thermal performance of solar cooker with the burnt oil and aluminum chips in outer and inner space respectively. The reason why burnt oil is used on the inner space is that, it is used as heat transfer fluid and also used as insulator during discharging period (due to its low thermal conductivity). Inside the solar cooker a pot is placed at the center. At the focal length of the upper parabola collector, an absorber with TES is provided upon which cooker is to be placed.

Figure 2 Prototype manufacturing and Assembly

2.4.3. Selection of sensible TES, reflector and insulation material

Based on the availability, cost, thermal conductivity, thermal diffusivity and environmental impact factors aluminum chips and burnt oil are selected for sensible TES. For its best reflectivity, cost, durability and other factors Aluminum foil is selected for reflecting material. Similarly, considering the availability, cost, thermal conductivity and diffusivity and impact on environment, for this thesis ash is selected for insulation material.

3. Results and Discussion

The experiments were made for a box-type solar cooker with an asymmetric CPC of horizontal aperture and an acceptance angle of 9.5^{o}. The internal box dimensions were 0.28 m per 0.24 m and 0.15 m high. The transparent double glazing of 4 mm thickness, 0.205 m height and 0.39 m width. The gap between the two glasses is 10 mm. The absorber plate, painted black, was made of aluminum sheet of a surface of 0.205m per 0.39m and 3mm thickness. The external box walls were made of mild steel sheet of 0.8 mm thickness and were insulated with ash of 50 mm thickness. The optical properties of the materials in the collector and the box cooker are listed in Table 1.

Table 1 Optical properties of materials in the cooker.

Parameter	Symbol	Value
Glass covers absorptivity	Av1 αv2	0.06
Glass covers transitivity	τ v1 τ v2	0.84
Glass covers emissivity	ε v1 ε v2	0.9
Glass covers reflectivity	ρ v1 ρ v1	0.05
Absorber plate absorptivity	αab	0.95
Absorber plate reflectivity	ρab	0.1
Absorber plate emissivity	εab	0.95

3.1. Experiment on the glazed glasses and absorber plates

The experiment is conducted for 7 consecutive hours from 10:00AM to 4:00PM. During the experiment the setup is planned and executed a set of experiments to achieve the required temperature on the upper glazed glass, inner glass and absorber plate. The temperature versus time result is shown in figure 3 shows the temperature result on 30 minutes interval of a total of 7 hours. The temperature is measured in kelvin and time is in minutes. Based on this a maximum temperature is achieved on the absorber plate and it was recorded as 598k (325.85°C). Similarly the temperature the maximum temperature recorded for the double glazed glasses become 424K (150.85°C) and 452K (178.85°C) for the outer and inner glasses respectively. This clearly indicates the absorptivity of the absorbing plate is functioning as required.

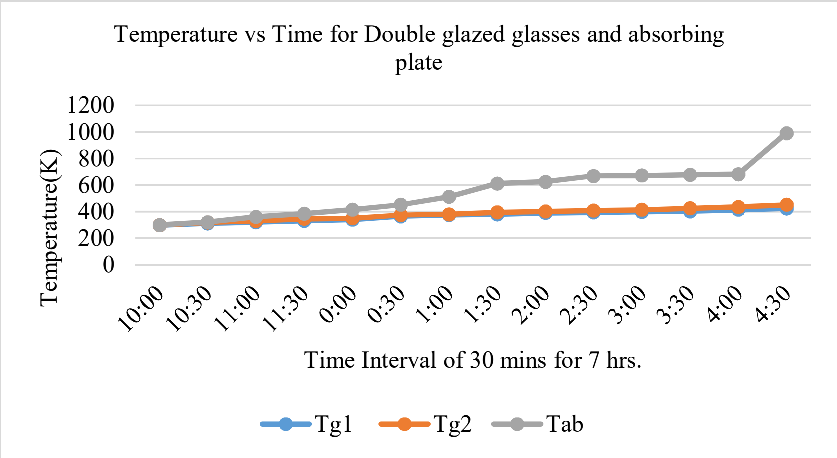

Figure 3 Time history of the Temperature for the double glazed glasses and absorbing plate

3.2. Experiment on Thermal Storage

Experiment on thermal storage container have been done to know how much time it will take to get the appropriate temperature to fry the potato chips. The experiment on the thermal storage materials i.e. the maximum temperatures recorded for the burnt oil, Aluminum chips, and cooking oil is 451K (177.85°C), 450K (176.85°C) and 443K(169.85°C) respectively on all the thermal storage materials as shown in the figure 4 The thermal storage spent 7 hours to get the maximum temperature (to charging). During charging period the graph shows that the temperature increment with time from 10:00AM to 4:00PM. The charging line shows little up and down, this is because of solar radiation variation due to time and wind effect. Thus as it is shown in figure 4 the temperatures–time history of the potato chips in the cooking pot, transferred from the thermal storage materials and to the cooking oil. When 1 kg of potato chips is fried by using the solar cooker for 20 minutes the required result was achieved.

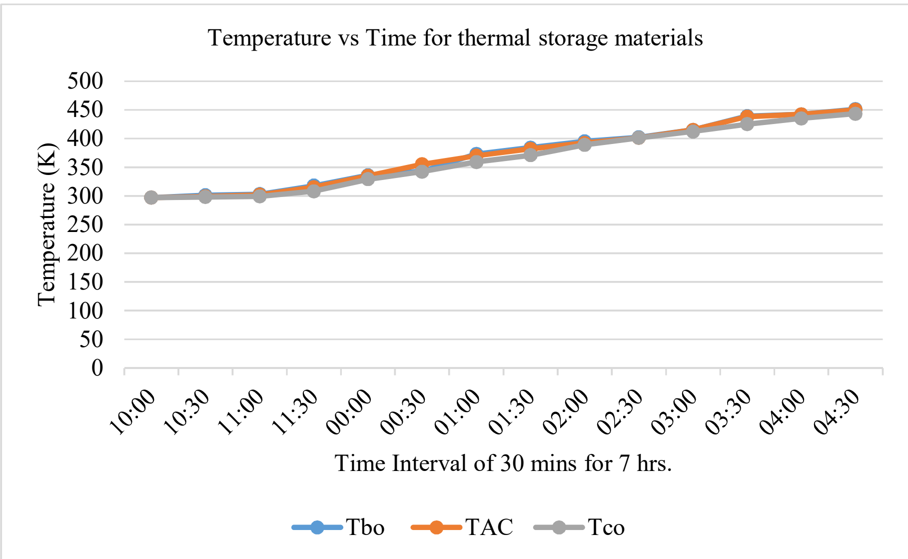

Figure 4 Time history of the thermal storage materials

3.3. Simulation Result

This MATLAB simulation is needed to show the temperature distribution on the absorber and to know how much energy is reached to the pot. According to the data listed in the appendix, the MATLAB software calculated all the equations above. The maximum temperature reached for the glass 1(outer) and glass 2 (inner) is 460k 396.05K (122.9°C) and 503.18(230°C) respectively, the absorber plate 720k (446.85°°C), the burnt oil 472.88K (199.73°C), Aluminum chips 472.84K (199.69°C) and cooking oil 471.85K (198.7°C).

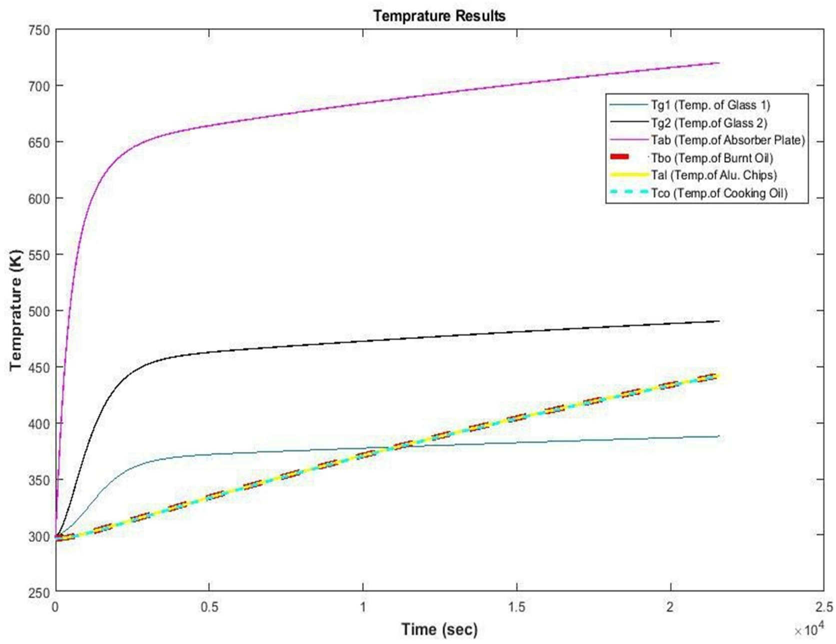

Figure 5 Output of the temperature versus time (MATLAB)

3.4. Performance of a solar cooker

3.4.1. The Stagnation Temperature Test

This test was performed in order to determine the first figure of merit of the cooker and associate it with the standard. The obtained value of $F1$ is (0.14w m2 w−1) and thus the soar cooker is marked as A- Grade since allowable standard $F1$ test conditions reveals that if the value of $F1$ is greater than 0.12, the cooker is marked as A-Grade and if $F1$ is less than 0.12 the cooker is marked as a B-Grade solar cooker (Folaranmi, 2013).

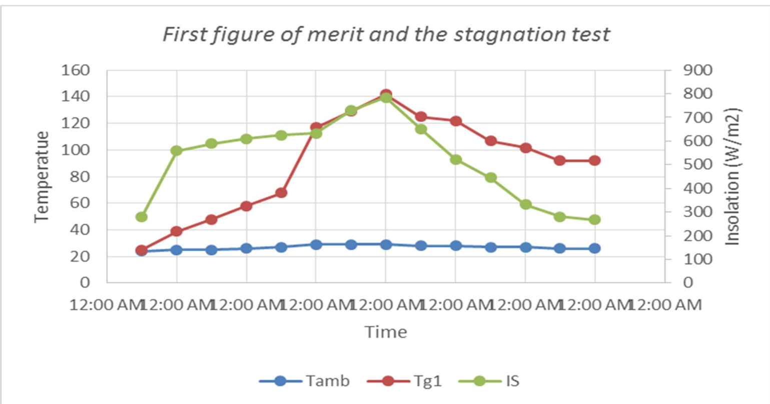

Figure 6 First figure of merit and the stagnation test

3.4.2. *Thermal Load Heat up Condition Test*

The solar box cooker was full with 1 kg of water at 30 ^{0} C in the solar cooking pot painted black; the water temperature was initially above the ambient temperature. Similarly the experimnet was conducted for 2kg and 3kg of water at 30^0 C .

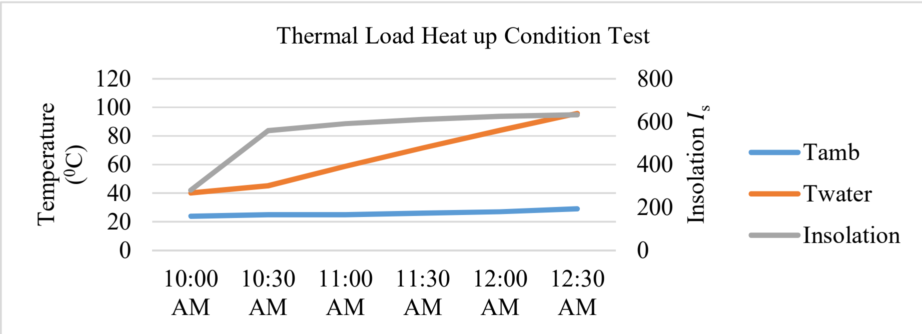

Figure 7 Thermal Load Heat up Condition Test

This experiment started by rising the water temperature (T_{w1}) step by step until it touches the maximum temperature or boiling point (T_{w2}). Selecting temperature for full load test, T_{w1} between the ambient temperature and boiling point and T_{w2} should be fixed in the temperature range 400C-950C. Take T_{wi}= 400C and T_{wf}= 930C. The suggested values of the second figure of merit are between the intervals of 0.254 to 0.49 (Folaranmi, 2013). The calculated value gained as 0.42, which is in between the recommended standard values. This indicates that, the solar cooker has a good heat transfer capacity.

3.4.3. *Cooking power test*

In continuation of the thermal load test the standard cooking power is analyzed. The cooking power experiments of the box-type solar cooker were conducted at 3 different days. The cooking vessel was filled with 1kg of water and the cooker was placed in the sun from 10:00 to 12:00. For the analysis, the test is conducted at an ambient temperature is between 20^{0}C - 35^{0}C, the test is conducted for a duration of 600seconds and solar radiation was taken from the Ethiopian Metrology data together with data obtained from internet. The initial and final water temperatures were chosen between 40^{0}C and 63.5^{0}C, for consecutive 120 minutes respectively. During the experimentation, the solar radiation, plate temperature, water temperature and ambient temperature were measured in 10-minute intervals

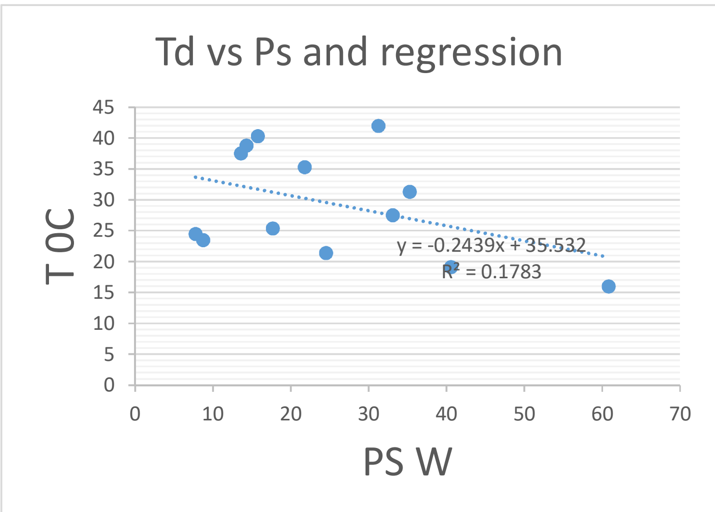

Figure 8 Standard cooking power of each interval against the temperature difference.

The general trend of the scatter diagram is that as temperature difference increases, standardized cooking power decreases. Correlation analysis shows that the correlation coefficient, R, was 0.42 and the coefficient of determination, R^2, was 0.1783. This means only about 17.83% of the variation of standardized cooking power can be attributed to temperature difference.

The standard cooking power for a 50 °C temperature difference was: Ps (50) = 29.10 W. The standard cooking power at 50ºC was calculated and tabulated in the table at 7:00 PM.

The standardized cooking power compared with another researcher's Zeleke Ademe and Sameer Hameer (Hameer, 25 January 2018)the standard cooking power at 50°C was 51W.

3.4.4. Efficiency Test

Fig. 9 shows the graph for efficiency as a function of average temperature above ambient. This gives optical efficiency, i.e., 86.31% as intercept and overall loss coefficient with 1.5% as negative of slope with the regression coefficient of 0.99.

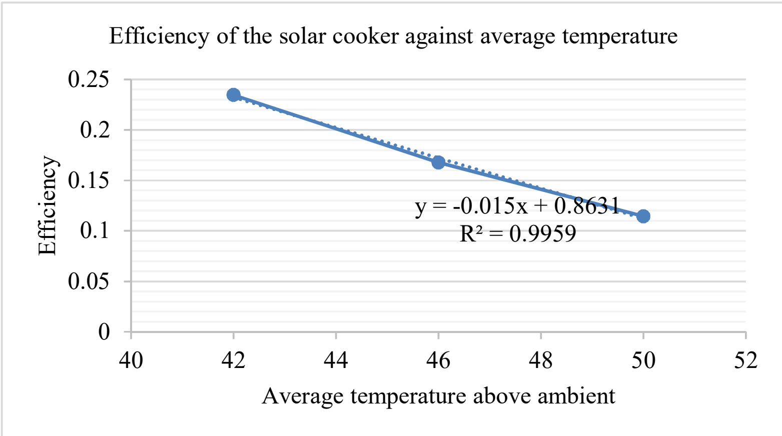

Figure 9 Efficiency of the solar cooker against average temperature

3.4.5. Economic evaluation of the cooker

Based on the data taken earlier the solar cooker with power rating 2500W is used to an electricity source and used for 4 hours, thus it consumes 10 kwh of energy. Based on the Ethiopian Electric utility (utility, 2023) tariff for those customers utilizing up to 300 kw/h is as of December 21,2023 Birr 2.00/kwh. Thus the annual cost of electricity is Birr 7,300.00.

Therefore, the payback period for the solar cooker, considering the given costs and savings, is approximately 1.837 years.

4. Conclusion

The research utilizes an asymmetric CPC material to develop a solar cooker, addressing the identified gap. The solar cooker design comprises an insulated box with parabolic reflectors, a vertical absorber plate, and a double-glazed cover. A prototype is constructed based on thermal balance equations and material selection. Experimental tests confirm successful gathering of solar radiation to achieve maximum temperatures on various components. A MATLAB simulation is conducted to compare results, showing close alignment between experimental and simulated values. However, discrepancies may arise from simplifications in the simulation, such as assumptions about air properties and solar radiation. The model validation and performance evaluation affirm the cooker as an A-Grade device with efficient heat transfer capabilities. Performance analysis indicates potential modifications for increased cooking power and efficiency. Economic analysis reveals a 2-year payback period for the system, factoring in material and labor costs, as well as economic variables. The construction process incorporates resourcefulness by utilizing materials like aluminum chips, burnt oil, and ash. Overall, the solar cooker demonstrates promising performance and economic viability, showcasing a successful integration of theoretical design and practical implementation.

5. References

A. Herez, M. R. (2018). Review on solar cooker systems: economic and environmental study for different Lebanese scenarios . *Renewable Sustainable Energy , 8*, 1421–432.

A. Veremachi, B. C. (2016). PCM heat storage charged with a double-reflector solar system. *Solar Energy* (2016).

A.A. Sagade, S. S. (2021). Enabling open sun cooling method-based estimation of effective concentration factor/ratio for concentrating type solar cookers. *Solar Energy , 227* , 568–576. .

A.G. Bhave, K. T. (2018). Development of a solar thermal storage cum cooking device using salt hydrate. *Solar Energy, 171* , 784–789.

A.H. Elsheikh, S. S. (2019). Modeling of solar energy systems using artificial neural network: a comprehensive review. *Solar Energy , 180* , 622–639. .

A.H. Tesfay, M. K. (2019). Numerical and experimental analysis of solar Injera baking with a PCM heat storage. *Journal of Science , 11*, 1–13. .

E.W. Gabisa, A. A. (2016). Characterization and experimental investigation of NaNO 3: KNO 3 as solar thermal energy storage for potential cooking application. *Solar Energy Engineering , 2016*, 1–6. .

Folaranmi, J. (2013). Performance Evaluation of a Double-Glazed Box-Type Solar Oven with Reflector. *Journal of Renewable Energy, 2013*, 1-9.

H. El Hage, A. H. (2018). An investigation on solar drying: a review with economic and environmental assessment. *Energy , 57* , 815–829.

H.A. Zafar, M. K. (2018). Introducing a novel design in the realm of box type solar cookers: an experimental study . *Renewable Sustainable Energy, 10*.

Hameer, Z. A. (25 January 2018). Design, construction and performance evaluation of aBox type solar cooker with a glazing wiper mechanism. *Energy* , 146–169.

MAWIRE, P. A. (2019). *SOLAR COOKERS WITH THERMAL ENERGY STORAGE: A SUSTAINABLE COOKING SOLUTION FOR DEVELOPING COUNTRIES.* SOUTH AFRICA: NORTH-WEST UNIVERSITY MAFIKENG CAMPUS.

Mohammadreza Sedighi, M. Z. (2014). A Review of Direct and Indirect Solar Cookers. *Sustainable Energy, 44-51*(No. 2), Vol. 2.

R. Wimmer, M. K. (2017). Analysis of user needs for solar cooker acceptance, in: Sustainability through Innovation in Product Life Cycle Design. *Springer*, 151–165.

S. Indora, T. K. (2018). Institutional cooking with solar energy: a review, . *Renewable Sustainable Energy Review, 84* , 131–154.

Senthil, R. (2020). Effect of charging of phase change material in vertical and horizontal rectangular enclosures in a concentrated solar receiver. *Jouranl of hermal Engieering* .

utility, E. e. (2023, January 24). *Ethiopian Electric Utility*. Retrieved from Ethiopian Electric Utility: http://www.ethiopianelectricutility.gov.et/electricity-tariff/detail/85?lang=en

V. Thirunavukkarasu, V. N. (2020). Experimental investigation on thermal performance of cavity receiver integrated with short term thermal energy storage for a solar parabolic dish concentrator. *Thermal Analysis. Calorim.* , 1–12.